EFFECT OF THERMAL AGING ON THE CORROSION BEHAVIOR OF WROUGHT AND WELDED ALLOY 22.

Raúl B. Rebak, Tammy S. Edgecumbe Summers and Tiangan Lian
Lawrence Livermore National Laboratory, Livermore, CA, USA

Ricardo M. Carranza
Comisión Nacional de Energía Atómica, Buenos Aires, Argentina

Jeffrey R. Dillman, Tina Corbin and Paul Crook
Haynes International Inc., Kokomo, IN, USA

ABSTRACT

Alloy 22 (UNS N06022) is a candidate material for the external wall of the high level nuclear waste containers for the potential repository site at Yucca Mountain. In the mill-annealed (MA) condition, Alloy 22 is a single face centered cubic phase. When exposed to temperatures on the order of 600°C and above for times higher than 1 h, this alloy may develop secondary phases that are brittle and offer a lower corrosion resistance than the MA condition. The objective of this work was to age Alloy 22 at temperatures between 482°C and 800°C for times between 0.25 h and 3,000 h and to study the corrosion performance of the resulting material. Aging was carried out using wrought specimens as well as gas tungsten arc welded (GTAW) specimens. The corrosion performance was characterized using standard immersion tests in aggressive acidic solutions and electrochemical tests in multi-component solutions. Results show that, in general, in aggressive acidic solutions the corrosion rate increased as the aging temperature and aging time increased. However, in multi ionic environments that could be relevant to the potential Yucca Mountain site, the corrosion rate of aged material was the same as the corrosion rate of the MA material.

Keywords: high-level nuclear waste, nickel-based alloy, N06022, aging, corrosion resistance, electrochemical behavior, immersion tests, ASTM G 28 A, hydrochloric acid, J-13 water, concentrated well water.

INTRODUCTION

Alloy 22 (UNS N06022) is a nickel-based alloy, which contains approximately 22% chromium (Cr), 13% molybdenum (Mo), 3% tungsten (W) and 3% iron (Fe). UNS N06022 has excellent resistance to pitting corrosion, crevice corrosion and stress corrosion cracking in halide containing environments.[1-11] Consequently, Alloy 22 is a candidate material to fabricate the external layer of the high level nuclear waste containers for the potential repository site in Yucca Mountain, Nevada.[12-13]

Due to the heat generated by the radioactive decay of the waste, the containers might experience temperatures as high as 160°C during their first 1000 years of emplacement. The lifetime design of the containers is 10,000 years. Previous studies have shown that the mechanical and corrosion properties of Alloy 22 did not change when it was aged for up to 40,000 h at 427°C.[4,6] However, it is known that precipitation of detrimental second phases occurs when Alloy 22 is aged at temperatures above 600°C.[13-19] The precipitation of these secondary phases that are formed at temperatures approximately 600°C and higher affect the corrosion resistance in aggressive acidic solutions and the mechanical properties of wrought Alloy 22.[13-19]

The purpose of this work was to study the effect of aging time and aging temperature on the corrosion behavior of Alloy 22 welds in aggressive acidic solutions. Similarly, this paper also addresses the effect of secondary phase precipitation on the anodic behavior of wrought Alloy 22 in multi-component electrolyte solutions that may result from evaporative experiments of ground waters from Yucca Mountain.[20]

EXPERIMENTAL TECHNIQUE

Three different sets of experiments are described in this paper. Two sets of experiments involve the use of wrought Alloy 22 and one set of experiments involved the use of welded Alloy 22 samples.

(1) For the first set of tests, samples of wrought Alloy 22 (heat 2277-6-3181) (Table 1) were aged in air for 1 h, 10 h, 100 h and 1000 h at 900°F (482°C), 1100°F (593°C), 1300°F (704°C) and 1472°F (800°C). These samples were used for electrochemical testing in J-13 water[21] (Table 2) at 95°C. The anodic behavior was determined using potentiodynamic polarization at a scan rate of 0.1 mV/s and the corrosion rate was evaluated using the AC Impedance technique. The impedance measurements were carried out potentiostatically by applying the corrosion potential with a sinusoidal perturbation of 10 mV amplitude, in a descending frequency scanning between 1 kHz and 1 mHz. The J-13 electrolyte solution was in the naturally aerated condition; that is, a gas was not purged through the solution during the tests but the ingress of air above the solution level was not restricted. The reference electrode was saturated calomel [SCE], which at room temperature is 0.240 V more positive than the normal hydrogen electrode (NHE). The samples were prismatic (modified ASTM G 5)[22] and were prepared from 0.25-inch (6.35 mm) thick plates. The sample finish was produced with wet silicon carbide paper 1200 mesh. The total exposed area was approximately 5 cm².

(2) In the second set of tests, wrought Alloy 22 samples (Heat 2277-8-3203) (Table 1) were aged in air for 10 h and 173 h at 700°C. These samples were used for cyclic polarization tests in simulated acidified water (SAW) and simulated concentrated water (SCW) solutions at 90°C (Table 2).[20] During the anodic

polarization, the scan rate was 0.167 mV/s. The electrolyte solutions were purged with air before and during the tests. The reference electrode was silver–silver chloride [SSC], which at room temperature is approximately 0.197 V more positive than the NHE. The samples were disks (ASTM G 5), which were prepared from 0.125-inch (3.2 mm) thick wrought sheet. They had a root mean square (RMS) roughness of 1 μ-inch and the total exposed area was approximately 0.7 cm^2.

(3) For the third set of tests, two 0.125-inch thick sheets of Alloy 22 (Heat 2277-9-3237) (Table 1) were welded using Alloy 22 filler metal (Heat 2277-8-3277) (Table 1). After welding the plates were sliced in strips approximately 0.5-inch wide. Each strip contained a weld seam in the center. The samples were aged for 0.25 h, 0.5 h, 1 h, 3 h, 6 h, 10 h, 30 h, 60 h, 100 h, 300 h, 600 h, 1000 h and 3,000 h at 900°F (482°C), 1000°F (538°C), 1100°F (593°C), 1200°F (649°C), 1300°F (704°C) and 1400°F (760°C). Aging was performed in air, and afterwards, the samples were rapid air-cooled. Most of the specimens were aged in the as-welded condition; however, one set of specimens was annealed at 2050°F (1121°C) for 20 minutes and water quenched before aging at 1200°F (649°C). The coupons for immersion testing contained by length approximately 1/3 of weld material and 2/3 of base material (1/3 at each side of the weld). Before testing the samples were cleaned by vapor blasting. Changes in the corrosion resistance were measured using standard immersion tests such as a boiling aqueous solution of 50% sulfuric acid (H_2SO_4) + 42 g/l of ferric sulfate ($Fe_2(SO_4)_3$) and boiling 2.5% hydrochloric acid (HCl). The first test solution is also called the Streicher test or ASTM G 28 A. This electrolyte boils at 120°C and is highly oxidizing. The second test solution is highly reducing, was carried out according to ASTM G 31 and it boils at approximately 101°C.[22] The ASTM G 28 A test was carried out for 24 h and the boiling HCl test was carried out for a total time of 96 h (the electrolyte solution was changed every 24 h). In these two tests, the solutions were open to the atmosphere through a condenser and a scrubber. Since the solutions were boiling, it is assumed that the amount of dissolved oxygen was insignificant.

RESULTS AND DISCUSSION

Corrosion Rate and Passive Behavior in Multi-Component Waters

J-13 Water. Figure 1 shows the polarization curves of Alloy 22 in J-13 water at 95°C for MA samples and for samples aged at 593°C and 800°C for 1000 h. At potentials more anodic than the corrosion potential, the polarization curves of the three materials showed a passive region of potentials with a corresponding current density of approximately 2 x 10^{-6} A/cm². Above this passive region, the three polarization curves showed an anodic peak followed by a second stage of passivation at a current density of 1 x 10^{-5} A/cm². The anodic peak occurred between 0.2 and 0.4 V [SCE] and had a maximum current density of approximately 3 x 10^{-5} A/cm². The breakdown potential occurred at approximately 0.5 V [SCE] for the sample aged at 800°C and at 0.65 V [SCE] for the MA sample and for the sample aged at 593°C. The increase of current density at the breakdown potential is likely to be a result of oxygen evolution and transpassive oxidation of Cr III to Cr VI. Figure 1 shows that there is no apparent effect of alloy aging on the passive behavior of Alloy 22 in J-13 water. That is, practically the same potential-current relationships were obtained for MA material and for aged materials.

Figure 2 shows typical Bode diagrams obtained for Alloy 22 at the corrosion potential in J-13 water at 95°C. These diagrams show typical capacitive behavior with a time distribution constant which can be represented by a constant phase element.[23] Electrochemical impedance measurements were carried out for MA annealed and aged materials at different times and temperatures. An equation that represents a

resistance-capacitance or RC equivalent circuit in parallel (Equation 1) was fitted to the experimental results

$$Z = R_{\Omega} + \frac{R_p}{1+(j\omega R_p C)^{\beta}} \qquad (1)$$

where R_{Ω} represents the resistance of the electrolyte solution between the surface of the specimen and the end of the Luggin capillary; that is, R_{Ω} is the ohmic component determined at high frequency. R_p represents the resistance determined at low frequency, which is associated to the resistance to polarization and is used to determine the corrosion rate of the alloy. β is the dispersion parameter, which indicates the deviation from an ideal circuit or model RC, C is the capacitance, ω is the angular frequency and j is the imaginary unit ($\sqrt{-1}$). Figure 3 shows the values of R_p for all the tested specimens. Figure 3 also shows the corrosion rate (CR) of Alloy 22 calculated from the values of R_p ($\Omega.cm^2$) according to Equation 2.

$$CR = \frac{EW}{\rho.F} \frac{b_a.b_c}{2.303(b_a+b_c)} \frac{1}{R_p} = \frac{201.83}{R_p} \left(\frac{mm}{year}\right) \qquad (2)$$

where EW is the equivalent weight of Alloy 22 (24.76 g/mol), ρ is the density of the alloy (8.69 g/cm^3), b_a and b_c are the anodic and cathodic Tafel slopes (0.1 V/decade of current) and F is the Faraday constant (96500 C/mol). Figure 3 shows that, under the tested conditions, the corrosion rate of Alloy 22 was approximately 2×10^{-4} mm/year and was not affected either by the aging temperature or the aging time. Similar results were also obtained in a solution containing 1000 ppm of sodium chloride (NaCl) represented by a full symbol. The scatter of the results in Figure 3 can be attributed to the low conductivity of the electrolyte solution ($R_{\Omega} = 500 \ \Omega.cm^2$) and the low current densities, which did not allow for measurements at frequencies below 1 mHz. In every case, the capacity value that was obtained from the fitting of the equation was in the order of 25 $\mu F.cm^{-2}$, which is the value expected for the capacity of the double layer. This also indicates that the passivating layer is very thin and that the value of its capacitance is also high, similar to the value expected for the double layer. Therefore, the values of capacitance measured experimentally corresponded to a combination in series of the capacitance of the oxide and the capacitance of the double layer.

It has been shown that when Alloy 22 was aged for 1000 h at 800°C, second detrimental phases formed not only at the grain boundary but also within the grains. Similarly, when Alloy 22 was aged at 593°C for 1000 h, partial grain boundary precipitation and long range ordering occurred.[18,19] It is likely that the precipitation of second phases, which greatly reduces the corrosion resistance of Alloy 22 in aggressive acidic solutions[13] are not detrimental for the corrosion behavior of Alloy 22 in milder environments that could be more representative of the potential repository site.

Anodic Behavior in Concentrated Waters. Figure 4 shows the anodic polarization curves of Alloy 22 in aerated SAW at 90°C. The polarization curves for MA material and for materials aged at 700°C for 10 h and for 173 h were similar. For all three aging conditions, the passive current density was approximately 4×10^{-6} A/cm², and the breakdown potential was approximately 0.65 V (SSC). It is assumed that the increase of current at the breakdown potential was a combination of oxygen evolution and the transpassive oxidation of chromium (Cr III to Cr VI). The Nernst equation for water of pH 2.8 and 90°C

predicts oxygen evolution of 10^{-6} atm at a potential in the vicinity of 0.7 V (SSC). A similar equation for Cr metal predicts the formation of 10^{-6} M chromate (CrO_4^{2-}) species (Cr VI) from Cr III species at a potential of 0.54 V (SSC).[24] Both of these values are in the vicinity of the breakdown potential of 0.65 V (SSC) reported above. For all three materials, the reverse curve of the cyclic polarization was similar or higher than the forward curve (Figure 4), indicating that Alloy 22 was not susceptible to localized corrosion in any of the tested conditions. Observation of the specimens after testing showed only general transpassive dissolution and the absence of crevice or pitting corrosion.

Figure 5 shows the anodic polarization curves of Alloy 22 in aerated SCW at 90°C. The polarization curves were similar for MA material and for materials aged at 700°C for 10 h and for 173 h. Each anodic polarization curve in Figure 5 had four characteristic regions. The first region was a passive current of approximately 1×10^{-5} A/cm², followed by a second region or anodic peak between the potentials of 0.2 V and 0.4 V (SSC). The maximum current density of this anodic peak was approximately 1×10^{-3} A/cm². The potential of the apex of the peak seemed to decrease slightly (~ 50 mV) as the aging time increased. The third region was a second passive segment at a current density of approximately 1×10^{-4} A/cm². The fourth was the transpassive region and it occurred at above approximately 0.7 V (SSC). For all three materials, the reverse curve was similar to the forward curve (Figure 5), indicating that Alloy 22 was not susceptible to localized corrosion in any of the tested conditions. Observation of the specimens after testing showed only general transpassive dissolution and absence of crevice and/or pitting corrosion.

Aging of wrought Alloy 22 for 10 h at 700°C produces partial grain boundary precipitation of detrimental second phases and aging for 173 h at 700°C produces full grain boundary coverage of this second phase.[18,19] It has been shown that the presence of secondary phases in Alloy 22 increased its critical current for passivation as well as the anodic passive current when anodically polarized in 1 M hydrochloric acid (HCl) solution at 66°C.[25] However, Figures 4 and 5 show that the presence of these secondary phases at the grain boundary do not affect the anodic behavior of Alloy 22 in concentrated multi component aqueous solutions that could be relevant to the potential repository site.

The anodic peak in Alloy 22 was only observed in near neutral and alkaline solutions (Figures 1 and 5) but it was not observed in an acidic solution (Figure 4). The maximum current density of this peak seemed to be approximately two orders of magnitude lower for a dilute solution (Figure 1) than for a concentrated solution of higher pH (Figure 5). Figure 1 and 5 also show that the current density in the second region of passivity (above the anodic peak) was one order of magnitude higher than the current density in the passive region below the peak. The origin and nature of this anodic peak are not fully understood yet; however, previous researchers attributed it to the oxidation of Mo IV to Mo VI.[26,27]

Immersion tests of welded material in aggressive acidic solutions

Table 3 shows the corrosion rates of welded Alloy 22 in ASTM G 28 A and boiling 2.5% HCl solutions for six aging temperatures and thirteen different aging times. Figures 6 shows that the corrosion rate of aged Alloy 22 in ASTM G 28 A solution (oxidizing) increased gradually as the aging time and the aging temperature increased (for T $\geq$ 538°C). For samples aged at 482°C the corrosion rate remained the same, even after aging for 3,000 h. For samples aged at 760°C and 704°C, the corrosion rate seemed to reach a plateau for aging times higher than 100 h. Observation of the tested coupons in the ASTM G 28 A solution showed preferential corrosion at the grain boundaries. At higher aging times deeper grain boundary

attack was observed, and in certain testing conditions some grains fell away because they became completely detached from the samples.

Figure 7 shows that the corrosion rate in boiling 2.5% HCl solution increased approximately three times after a certain threshold aging time at each temperature. The higher the temperature the lower the threshold time. Corrosion data for 760°C and 704°C shows that after this initial sudden increase in the corrosion rate, it remained approximately constant as the aging time increased; however, it increased again after a second threshold time. For samples aged at 482°C the corrosion rate remained the same, even after aging for 3,000 h. Observation of the tested coupons in boiling 2.5% HCl solution showed preferential intergranular attack which became deeper and wider as the aging time increased. At aging times of 1000 h and higher, preferential corrosion attack at twins inside the grains was observed.

Figures 8 and 9 show the effect of annealing on the corrosion behavior of Alloy 22 welded coupons. Figure 8 shows the corrosion rate in ASTM G 28 A for a series of coupons that were aged in the as welded conditions and also for coupons that were annealed at 1121°C for 20 minutes and then water quenched before aging. For aging times shorter that 10 h the corrosion rate of the annealed coupons was higher than of those that were in the as-welded conditions (Figure 8). For aging times of 10 h and 30 h, the corrosion rate of both types of coupons was the same; however, for aging times of 60 h to 1000 h, the corrosion rate of the annealed coupons was lower than the corrosion rate of the as-welded coupons. This behavior is not fully understood. On the other hand, Figure 9 shows that in boiling 2.5% HCl solution, the corrosion rate of the annealed and aged coupons was always lower than the corrosion rate of the as-welded and aged coupons.

Figures 10 and 11 show the effect of welding on the corrosion rate of Alloy 22. Most of the corrosion rates of wrought Alloy 22 were published before.[13,27] Figure 10 shows the corrosion rate in ASTM G 28 A for wrought and as-welded coupons at two aging temperatures (760°C and 538°C) as a function of aging time. For all aging times, the corrosion rate of welded coupons was always higher than the corrosion rate of wrought coupons. For example, at the aging temperature of 760°C and at the aging time of 10 h, the corrosion rate of the welded coupons was approximately two times the corrosion rate of the wrought coupons. Figure 11 shows the corrosion rate in boiling 2.5% HCl solution for wrought and as-welded coupons at two aging temperatures (760°C and 538°C) as a function of aging time. For all aging times, the corrosion rate of welded coupons was always higher than the corrosion rate of wrought coupons. For the shorter aging times (up to 3-6 h) the corrosion rate of the welded coupons was approximately three times the corrosion rate of the wrought coupons; however, for aging times of 6 h and longer, the difference in the corrosion rate was smaller.

Figure 12 shows the time necessary at each aging temperature for Alloy 22 to reach a corrosion rate of 80 mpy (~ 2 mm/year) in ASTM G 28 A, both for wrought and welded materials. Figure 12 shows that at each aging temperature, a shorter aging time is required for the welded material to reach the threshold corrosion rate of 80 mpy (Figures 10). Figure 12 shows that the Arrhenius slopes for both materials are the same, that is, the degradation of the welded material started earlier than the degradation for the wrought material; however, the degradation rate was the same. The slope of both curves in Figure 12 could be equated to $-Q_{ap}/R$, where Q_{ap} is the apparent activation energy for the aging process in Alloy 22 and R is the gas constant. Calculations show that this apparent activation energy, as determined by corrosion testing in oxidizing conditions (ASTM G 28 A) was 261 kJ/mol for wrought material and 262 kJ/mol for welded material. A similar plot for corrosion in boiling 2.5% HCl (reducing conditions) showed Q_{ap} = 244 kJ/mol for wrought material and Q_{ap} = 306 kJ/mol for welded material. For the 2.5%

HCl solution, the curves for both materials were not parallel as in the case of the ASTM G 28 A solution. Assuming that the aging mechanism remains the same at the lower temperatures, Figure 12 shows that if the Arrhenius relationship is extrapolated to aging temperatures of 300°C, aging times higher than 10,000 years would be necessary for Alloy 22 to show a degradation corresponding to a corrosion rate of 80 mpy.

CONCLUSIONS

(1) The corrosion rate of MA and aged Alloy 22 in simulated J-13 water at 95°C was in the order of 0.0002 mm/year and it did not change as a function of aging temperature and aging time.

(2) Cyclic polarization curves of MA and aged Alloy 22 in aerated SAW and SCW multi component solutions at 90°C were the same.

(3) When anodically polarized in near neutral and alkaline solutions, both MA and aged Alloy 22 showed an anodic peak between 0.2 V and 0.4 V (SSC). This peak was not evident in acidic solutions.

(4) When welded Alloy 22 coupons were aged at temperatures between 538°C and 760°C, the corrosion rate in oxidizing (ASTM G 28 A) and reducing (boiling 2.5% HCl) solutions increased both with the aging temperature and aging time.

(5) For the same aging temperature and aging time, the corrosion rate of welded Alloy 22 was higher than the corrosion rate of wrought material.

(6) The corrosion degradation rate of Alloy 22 due to high temperature aging was the same for wrought and welded materials.

ACKNOWLEDGMENTS

DISCLAIMER

sarily state or reflect those of the United States Government or the University of California, and shall not be used for advertising or product endorsement purposes.

REFERENCES

1. P. E. Manning, J. D. Schöbel, Werkstoffe und Korrosion, 37, (1986): p 137.
2. A. I. Asphahani, The Arabian Journal for Science and Engineering, Volume 14, Number 2, (1989): p. 317.
3. S. J. Lukezich, The Corrosion Behavior of Ni-Base High Performance Alloys in Simulated Repository Environments, MS Thesis, The Ohio State University, 1989.
4. R. B. Rebak, in Proceedings of the Symposium on Passivity and Its Breakdown, Volume 97-26 (Pennington, NJ: The Electrochemical Society, 1998): p. 1001
5. A. K. Roy, D. L. Fleming, B. Y. Lum, MP, March, (1998): p. 54.
6. R. B. Rebak and N. E. Koon, Corrosion/98, Paper 153, (Houston, TX: NACE International, 1998).
7. K. A. Gruss, G. A. Cragnolino, D. S. Dunn, N. Sridhar, Corrosion/98, Paper 149 (Houston, TX: NACE International, 1998).
8. R. B. Rebak, P. Crook, in Critical Factors in Localized Corrosion III, Volume PV 98-17 (Pennington, NJ: The Electrochemical Society, 1999): p. 289.
9. R. B. Rebak, N. E. Koon, J. P. Cotner, P. Crook, in Passivity and Localized Corrosion, Volume PV 99-27 (Pennington, NJ: The Electrochemical Society, 1999): p. 473
10. D. S. Dunn, G. A. Cragnolino, N Sridhar, in Scientific Basis for Nuclear Waste Management XXII, Vol. 556 (Warrendale, PA: Materials Research Society, 1999): p. 879.
11. B. A. Kehler, G. O. Ilevbare, J. R. Scully, Corrosion/2000, Paper 182 (Houston, TX: NACE International, 2000).
12. D. S. Dunn, G. A. Cragnolino, N Sridhar, in Scientific Basis for Nuclear Waste Management XXIII, Vol. 608 (Warrendale, PA: Materials Research Society, 2000): p. 89.
13. R. B. Rebak, N. E. Koon, J. R. Dillman, P. Crook, T. S. Edgecumbe Summers, Corrosion/2000, Paper 181 (Houston, TX: NACE International, 2000).
14. S. J. Matthews in Proceedings of the Third International Conference on Superalloys, (Baton Rouge, LA: Claitor's Publishing Division, 1976): p. 215.
15. U. L. Heubner, E. Altpeter, M. B. Rockel and E. Wallis, Corrosion, 45 (1989): p. 249.
16. H. M. Tawancy, J. Mater. Sci., 31 (1996): p. 3929.
17. T. S. Edgecumbe Summers, M. A. Wall, M. Kumar, S. J. Matthews, R. B. Rebak, in Scientific Basis for Nuclear Waste Management XXII, Vol. 556 (Warrendale, PA: Materials Research Society, 1999): p. 919.
18. R. B. Rebak, T. S. Edgecumbe Summers, R. M. Carranza, in Scientific Basis for Nuclear Waste Management XXIII, Vol. 608 (Warrendale, PA: Materials Research Society, 2000): p. 109.
19. T. S. Edgecumbe Summers, T. Shen, R. B. Rebak in Ageing Studies and Lifetime Extension of Materials, (New York, NY: Kluwer Academic/Plenum Publisher, 2001): p. 507
20. N. D. Rosenberg, G. E. Gdowski and K. G. Knauss, Applied Geochemistry, 16 (2001), p. 1231
21. J. E. Harrar, J. F. Carley, W. F. Isherwood and E. Raber, Report on the Committee to Review the use of J-13 Well Water in Nevada Nuclear Waste Storage Investigations, LLNL UCID 21867 (University of California, January 1990).
22. Annual Book of ASTM Standards, Volume 03.02 (West Conshohocken, PA: American Society for Testing and Materials, 2001).

23. J. Ross Macdonald, Impedance Spectroscopy – Emphasizing Solid Materials and Systems, (New York, NY: John Wiley and Sons, 1987).
24. M. Pourbaix, Atlas of Electrochemical Equilibria in Aqueous Solutions (Houston, TX: NACE International, 1974).
25. R. B. Rebak, N. E. Koon, P. Crook, in Electrochemical Approach to Selected Corrosion and Corrosion Control Studies, Number 28 (London, UK: The Institute of Materials, 2000): p. 245
26. J. Postlethwaite, R. J. Scoular and M. H. Dobbin, Corrosion, 44 (1988): p. 199.
27. G. O. Ilevbare, T. Lian and J. C. Farmer, "Environmental Considerations in the Studies of Corrosion Resistant Alloys for High-Level Radioactive Waste Containment," CORROSION/02, Paper no. 539 (Houston, TX: NACE International, 2002).

TABLE 1

CHEMICAL COMPOSITION OF THE STUDIED ALLOY 22 HEATS (WT%)

Element	2277-6-3181	2277-8-3203	2277-9-3237	2277-8-3277
C	0.004	0.002	0.0047	0.0066
Co	1.11	1.82	0.9	1.1
Cr	21.59	21.3	21.26	21.58
Fe	3.9	4.0	3.97	4.17
Mn	0.28	0.19	0.25	0.25
Mo	13.64	13.08	13.15	13.29
Ni	~56.3	~56.5	~57.4	~56.3
P	0.013	<0.005	0.01	0.005
S	<0.001	0.008	0.003	0.0031
V	0.17	0.14	0.21	0.18
W	3.03	2.93	2.90	3.18

TABLE 2

CHEMICAL COMPOSITION OF MULTIIONIC ELECTROLYTE SOLUTIONS (mg/L)

Ion	J-13, pH 7.4	SCW, pH 10.3	SAW, pH 2.8
K^+	5.04	3400	3400
Na^+	45.8	40,900	40,900
Mg^{2+}	2.01	< 1	1000
Ca^{2+}	13	< 1	1000
F^-	2.18	1400	0
Cl^-	7.14	6700	24,250
NO_3^-	8.78	6400	23,000
SO_4^{2-}	18.4	16,700	38,600
HCO_3^-	128.9	70,000	0
SiO_3^{2-}	61.1	~ 40	~ 40

TABLE 3
CORROSION RATE OF WELDED AND WELDED + AGED ALLOY 22 IN MPY
To convert mpy to mm/year multiply by 0.0254

Aging Temp. °C (°F)	Aging Time, h	ASTM G 28 A	2.5% HCl, boiling
Ambient	Variable	41.3, 44.1	214, 215
760 (1400)	0.25	65.2, 65.1	611, 602
	0.5	75.9, 75.7	691, 697
	1	97, 97.5	759, 737
	3	192, 175	746, 745
	6	280, 246	715, 704
	10	321, 337	711, 710
	30	555, 609	701, 715
	60	609, 720	792, 755
	100	719, 721	806, 769
	300	958, 932	881, 868
	600	1115, 1074	910, 862
	1000	1181, 1162	856, 853
704 (1300)	0.25	39.1, 38.8	247, 257
	0.5	44.7, 49.8	290, 295
	1	50.6, 53.5	324, 329
	3	73.4, 51.2	511, 504
	6	119, 124	705, 690
	10	123, 126	722, 708
	30	300, 304	704, 725
	60	602, 611	683, 686
	100	732, 742	670, 690
	300	1318, 1385	758, 784
	600	1423, 1424	850, 848
	1,000	1130, 1123	901, 916
649 (1200)	0.5	40, 38.6	198, 196
	1	40.7, 39.8	212, 199
	3	40.7, 39.6	214, 213
	6	40.4, 42.3	243, 238
	10	57.1, 56.3	249, 280
	30	79.2, 74.9	427, 390
	60	97.2, 92.2	597, 628
	100	119, 114	670, 642
	300	366, 348	692, 682
	600	896, 1221	695, 675
	1,000	2064, 2077	728, 709

649 (1200)	0	58.3, 63.5	147, 147
ASW + Annealed	0.5	70.2, 73.4	150, 146
at 2050°F (1121°C)	1	55.7, 51.4	156, 156
for 20 Minutes	3	66.7, 64.8	158, 152
+ Water Quenched	6	45.4, 49.1	154, 170
Before Aging	10	56.1, 62.3	166, 153
	30	69.5, 71.6	222, 205
	60	68.6, 76.3	493, 502
	100	70.5, 75.8	529, 545
	300	207, 165	609, 600
	600	289, 307	573, 615
	1,000	447, 567	608, 631
593 (1100)	0.5	49, 49.8	207, 207
	1	46.2, 46.2	198, 205
	3	46.6, 46.5	200, 202
	6	45.3, 47.4	214, 206
	10	47.6, 48.4	225, 214
	30	48.6, 49.5	201, 209
	60	47.5, 43.8	210, 214
	100	52.8, 54	220, 217
	300	68.7, 71.5	322, 319
	600	98.8, 92.7	494, 504
	1,000	120, 118	586, 585
538 (1000)	1	52.1, 53.1	245, 260
	3	51.8, 50.5	253, 253
	6	50, 53.2	253, 262
	10	53.7, 55.8	180, 189
	30	47.4, 45.6	189, 193
	60	38.7, 39.8	200, 196
	100	44.5, 44	202, 184
	300	32.4, 36.2	222, 230
	600	46.1, 45.4	259, 254
	1,000	48.1, 48.5	261, 288
	3,000	87, 88.5	473, 487
482 (900)	1	54.7, 55	206, 202
	3	56.4, 53.2	196, 195
	6	52.5, 53.7	202, 191
	10	53.1, 52.7	201, 193
	30	50.9, 50.5	190, 187
	60	40.5, 41.5	189, 183
	100	38.8, 42.4	199, 189
	300	39.8, 39.5	188, 192
	600	44.8, 44.4	188, 192
	1,000	45.6, 45.4	233, 255
	3,000	34.1, 35.3	179, 179
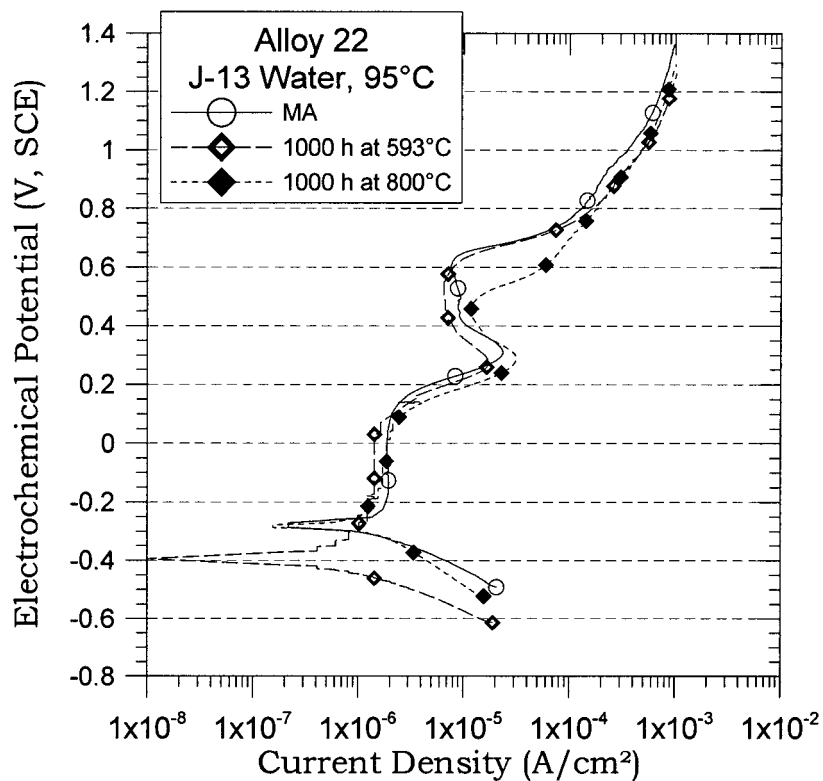
FIGURE 1: Polarization curves of Alloy 22 in J-13 Water at 95°C
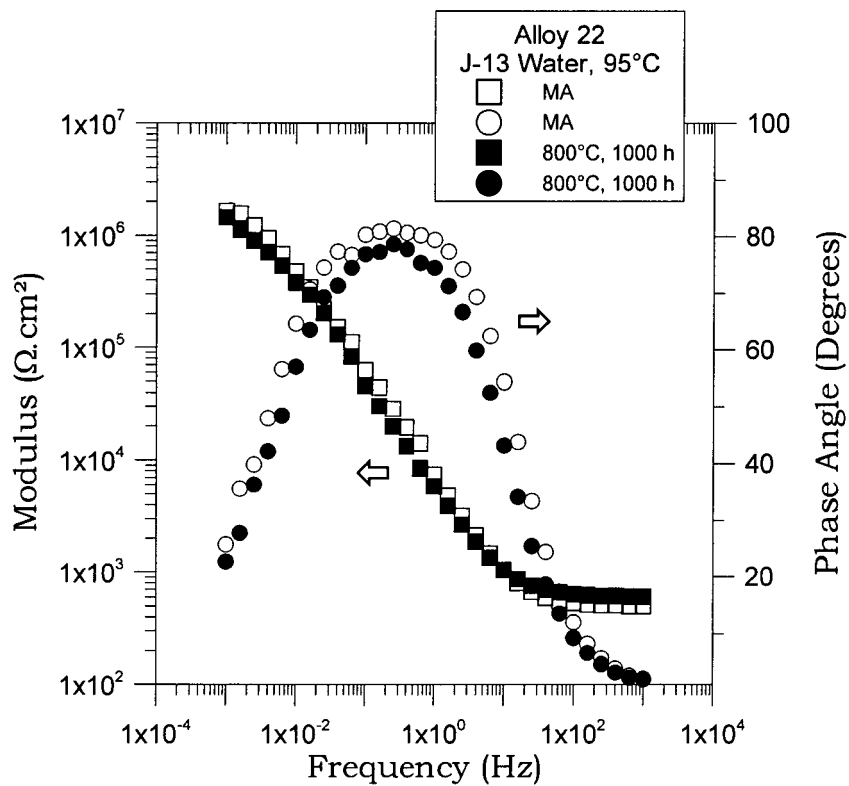
FIGURE 2: Typical Bode diagrams for Alloy 22 in J-13 Water at 95°C.
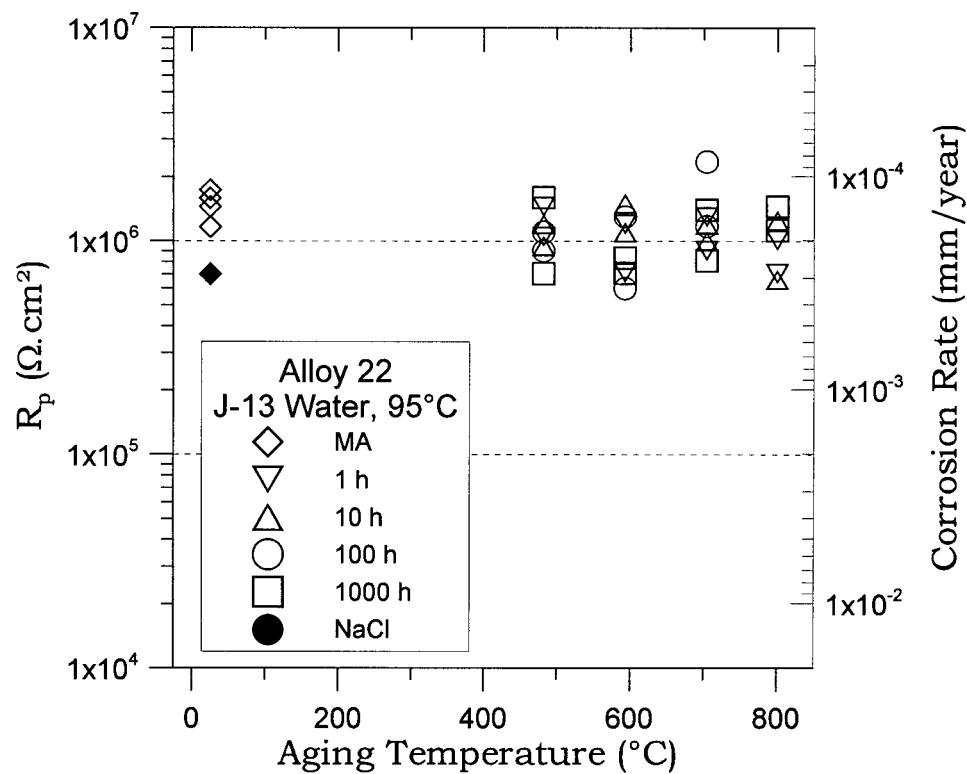
FIGURE 3: Corrosion rate of Alloy 22 in J-13 water as a function of aging temperature and aging time.
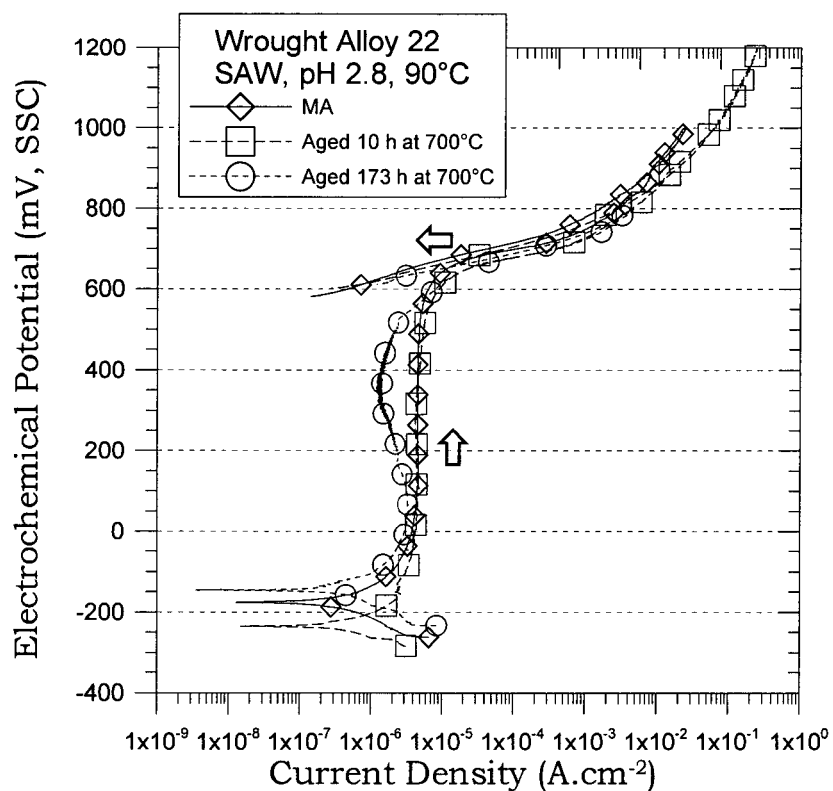
FIGURE 4: Cyclic polarization curve of Alloy 22 in SAW at 90°C.
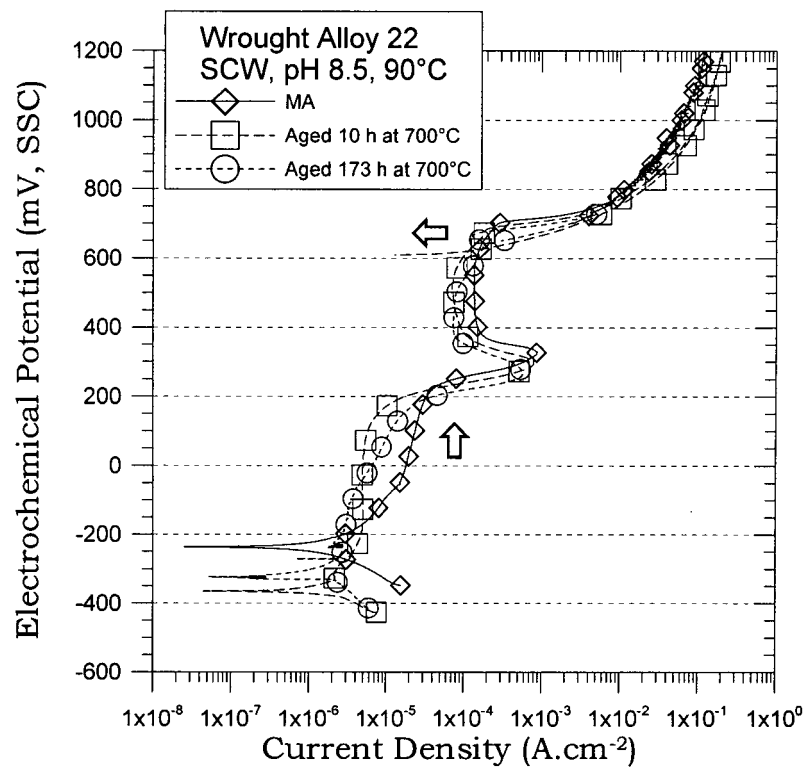
FIGURE 5: Cyclic polarization curves of Alloy 22 in SCW at 90°C.
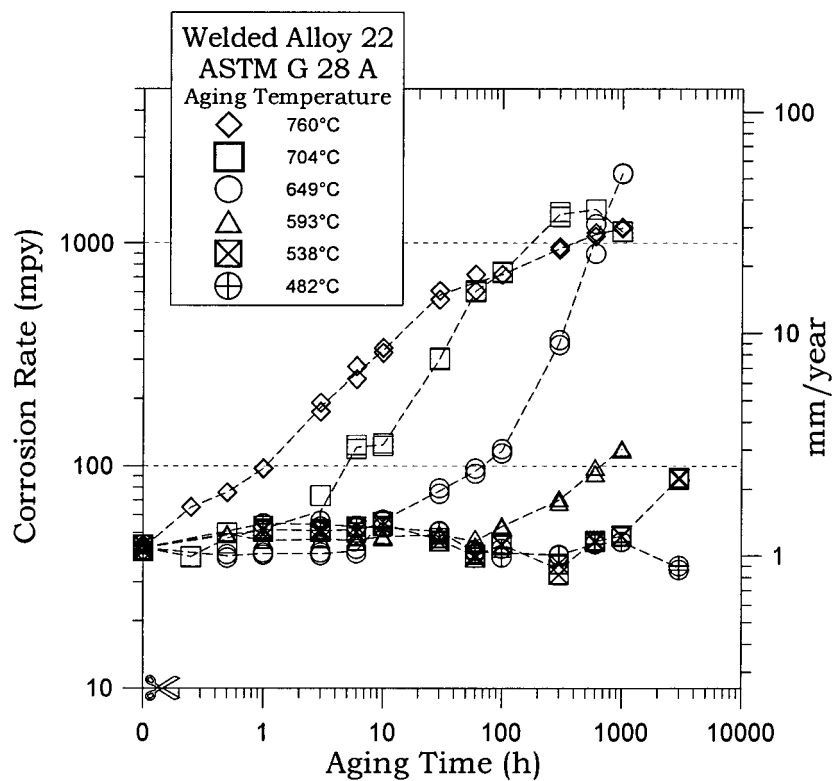
FIGURE 6: Corrosion rate of As-Welded and Welded + aged Alloy 22 in ASTM G 28 A solution.
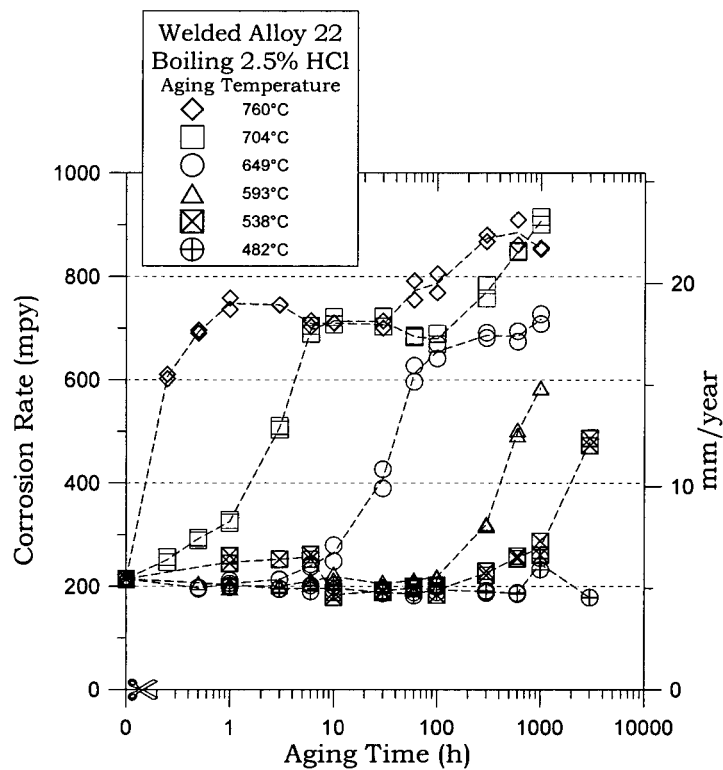
FIGURE 7: Corrosion rate of As-Welded and Welded + aged Alloy 22 in boiling 2.5% HCl solution.
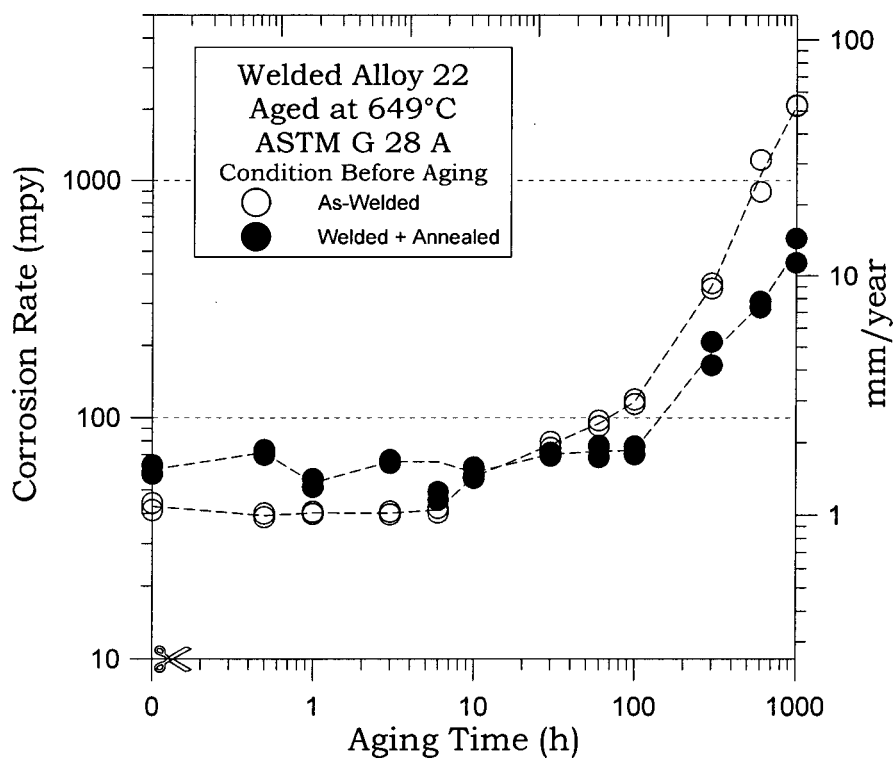
FIGURE 8: Corrosion rate in ASTM G 28 A solution of As-Welded and Welded + annealed Alloy 22 aged at 649°C.
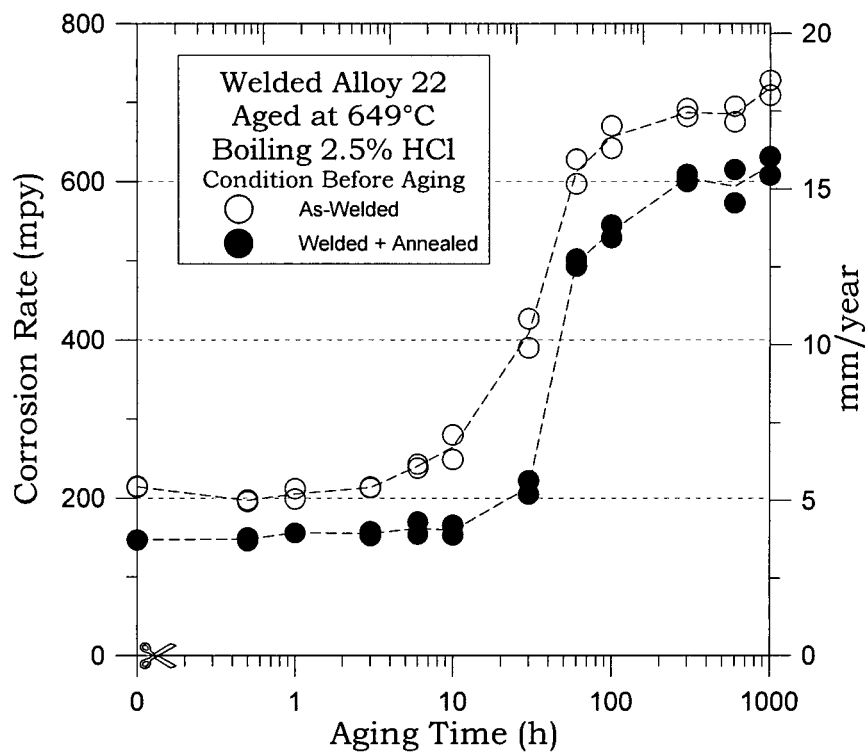
FIGURE 9: Boiling 2.5% HCl solution of As-Welded and Welded + annealed Alloy 22 aged at 649°C.
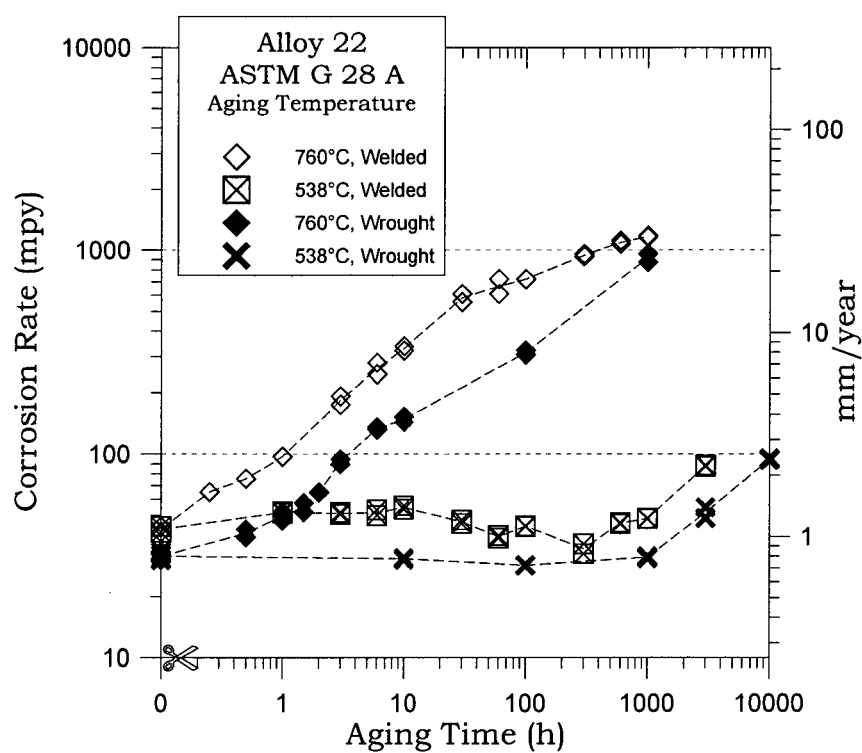
FIGURE 10: Corrosion rate in G 28 A solution for wrought and welded Alloy 22.
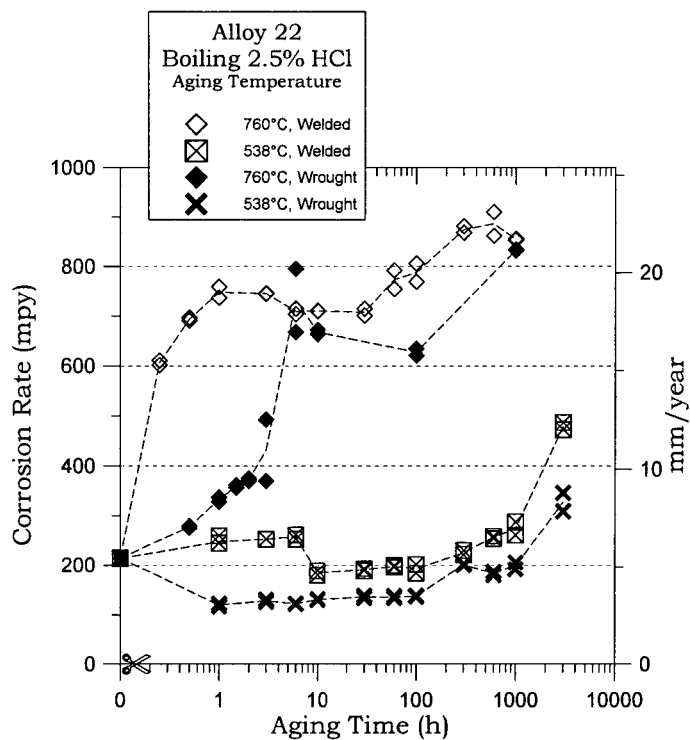
FIGURE 11: Corrosion rate in boiling 2.5% HCl solution for wrought and welded Alloy 22.
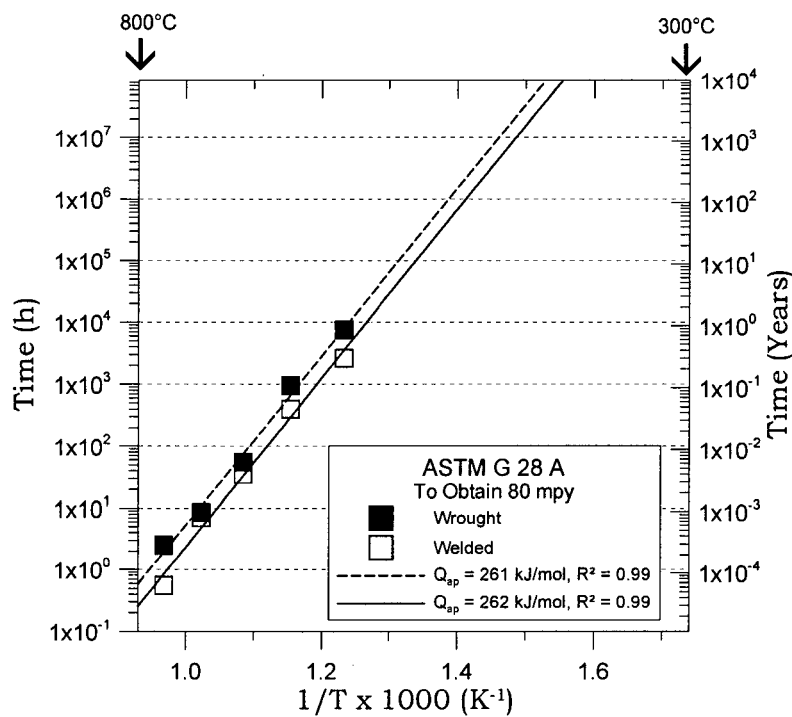
FIGURE 12: Arrhenius extrapolation for the corrosion behavior of wrought and welded Alloy 22.

Effect of Thermal Aging on the Corrosion Behavior of Wrought and Welded Alloy 22

R.B. Rebak, T.S. Edgecumbe Summers, T. Lian, R.M. Carranza, J.R. Dillman, T. Corbin, P. Crook

U.S. Department of Energy

Lawrence
Livermore
National
Laboratory

January 2, 2002